Astron. Astrophys. 363, 323–334 (2000)

ASTRONOMY AND ASTROPHYSICS

Active regions on the surface of Comet 43P/Wolf-Harrington determined from its nongravitational effects

S. Szutowicz

Space Research Centre of the Polish Academy of Sciences, Bartycka 18A, 00-716 Warsaw, Poland (slawka@cbk.waw.pl)

Received 31 May 2000 / Accepted 6 July 2000

Abstract. The nongravitational perturbations in the motion of the periodic comet Wolf-Harrington are investigated during its nine observable apparitions in the period 1924–1998. To explain the irregular variations in the nongravitational acceleration, two different models are considered and successfully used to link all the apparitions: a) Model of nucleus with the activation and deactivation of discrete outgassing sources on the surface; b) Forced precession model of the spin axis of the nucleus with an activity described by nonlinear changes of the perihelion shift of the gas production curve.

The first model is represented by two slightly different orbital solutions in which the northern active region is persistent and the initiations and disappearances of two southern regions are responsible for the observed variability of the nongravitational acceleration. Profiles of the modelled gas production rates are compared with observed light curves of the comet and used for an estimation of the effective outgassing area and the activity level of the cometary nucleus. According to all employed models of the nongravitational acceleration similar shifts of the maximum of the comet activity with respect to successive perihelion passages over the whole examined interval of the motion have been detected.

The model parameters describing physical properties of the comet nucleus such as the nucleus orientation, the localization and the size of the active regions or the oblateness of the nucleus are derived from numerical fitting of the models to positional observations of the comet.

Key words: comets: individual: 43P/Wolf-Harrington

1. Introduction

A faint comet, discovered photographically as a $16th$ magnitude object on 1924 December 22 by M. Wolf at Heidelberg, was observed only for about one month. The following three successive returns of the comet to the Sun were lost for observations. After twenty seven years in October 1951 it was again rediscovered at Mt. Palomar Observatory by R. G. Harrington. The discovery was not immediately suspected as the return of Wolf's comet. The identity of both comets has been proved after the 1957 apparition (Wiśniewski 1964). With an orbital period of about 6.5 years, the Comet Wolf-Harrington belongs to the Jupiter family comets. The comet is in a chaotic orbit and approached Jupiter twice in 1936 and in 1948 what caused considerable changes in orbital parameters, especially in the perihelion distance and the eccentricity. Since 1952 it has been observed at every eighth return to perihelion.

The existence of a nongravitational anomaly in the comet motion between 1951 and 1965 has been noted by Sitarski (1970) and next confirmed by Marsden (1977) by linking observations from four apparitions. To link observations from the period 1951–1977 Sitarski (1981) assumed a constant secular change of the semi-major axis of the comet's orbit. The nongravitational acceleration over ten returns of the comet to the Sun, from 1924 to 1985, was investigated by Szutowicz (1987). It appeared that the motion of the comet is affected by variable nongravitational effects and an essential change of their pattern occured after 1978. The observations from seven comet's apparitions covering the period 1951–1991 were successfully linked assuming a linear precession of the cometary spin axis (Szutowicz 1992). However, the model seemed to be nonphysical because of extremaly fast rate of precession, especially in the angle related to the longitude of the Sun.

In the present paper the more detailed analysis of the nongravitational acceleration in the motion of comet 43P/Wolf-Harrington during its all apparitions is performed. The irregular character of the comet's nongravitational perturbations has been explained by changes in a surface distribution of the active areas (Sect. 4.4) and by a forced precession of the spin axis coupled with nonlinear shifts of the function $g(r)$ with respect to the perihelion time (Sect. 4.3). Sect. 6.2 contains estimations of the effective active area. In Sect. 7 the size of the nucleus radius on the basis of orbital models and photometric observations is discussed.

2. Modelling of the nongravitational acceleration

The nongravitational acceleration observed in the motion of periodic comets is due to the momentum transferred to the nucleus by the anisotropic outgassing. When a comet approaches the Sun the heating of a nucleus surface by solar radiation causes sublimation of its icy layers. Nongravitational forces cannot be accurately predicted by theoretical analysis because of difficulty in

modelling such factors as a nonspherical shape of nuclei, surface topography, distribution of icy areas exposed for vaporization, or inhomogeneity of cometary material.

In the standard model of nongravitational acceleration it is assumed that the whole surface of a rapidly rotating and smooth spherical cometary nucleus undergoes sublimation of the water snow. Marsden et al. (1973) introduced a method of determination of the nongravitational effects in the orbital investigations. According to this method the nongravitational terms are directly included into the equations of a comet's motion:

$$\ddot{\mathbf{r}} + k^2 \frac{\mathbf{r}}{r^3} = \frac{\partial R}{\partial \mathbf{r}} + a_1 \frac{\mathbf{r}}{r} + a_2 \frac{r\dot{\mathbf{r}} - \dot{r}\mathbf{r}}{h} + a_3 \frac{\mathbf{h}}{h}, \qquad (1)$$

where $\mathbf{r}$ is the radius vector, k is Gaussian gravitational constant, R is the planetary disturbing function, and vector $\mathbf{h}$ is defined by $\mathbf{h} = \mathbf{r} \times \dot{\mathbf{r}}$. The orbital components of the nongravitational acceleration in the radial, transverse and normal direction are a_1, a_2 and a_3, respectively. In the Marsden's formalism, they are given by: $a_i = A_i\ g(r),\ \ (i = 1, 2, 3)$, where the constants A_i can be determined along with orbital elements from the least square fit to positional observations of a comet. The positive value of transverse component indicates an additional deceleration in a comet's motion. Likewise, a nongravitational acceleration is associated with negative value of the transverse component. The value of the nongravitational force is changing with heliocentric distance of a comet, r, according to symmetric with respect to the perihelion function $g(r)$ which simulates the ice water sublimation rate. An existence of nonradial terms of the nongravitational force is connected with rotation of the comet nucleus.

For a cometary nucleus rotating around a fixed axis, Sitarski (1990) developed a procedure to treat the nongravitational parameters as functions of time:

$$A_i(t) = A\ C_i\left(\eta, I, \lambda_\odot\right), \quad i = 1, 2, 3, \qquad (2)$$

where the argument of the Sun is: $\lambda_\odot = v(t) + \phi$. The solar longitude at the perihelion ϕ is measured along the orbit from its ascending node on the equator in the sense of increasing true anomaly $v(t)$ of the comet. The angle I is the obliquity of the orbit plane to the nucleus equator and η is the lag angle of the outgassing maximum behind the subsolar meridian. The formulae for direction cosines C_i have been introduced by Sekanina (1981). The parameters: A, η, I and ϕ are determined from the observational equations of a comet in an iterative process of the orbit improvement.

Both, the standard model of the nongravitational acceleration and the model with the angular parameters, were used to investigate the motion of 43P/Wolf-Harrington in intervals of time covering either three or four of its returns to the Sun (Sect. 4.1).

A long-term variation of the nongravitational effects detected in the motion of some short-period comets can be interpreted in terms of spin axis precession. Quantitative model of the forced precession of the nuclear spin axis has been derived by Whipple & Sekanina (1979) to explain observable temporal variations in the nongravitational motion of the comet 2P/Encke. Then the model was developed and applied to comets with a strange behaviour of A_2 (Sekanina 1984, 1985a, 1985b, Sekania & Yeomans 1985). According to the forced precession model, nonlinear variations with time of the direction of the spin axis are caused by changes in the reactive force acting on the nonspherical nucleus. The precession rate is a function of: the lag angle, η, the nucleus orientation defined by angles I and ϕ, the modulus of the reactive force, the nucleus oblateness, s, and the precession factor, $f_{\rm p}$, which depends on a rotational period and a nucleus size. The forced precession model was adopted for orbital computation i.e. the precession formulae were transformed in such a way to include them directly into equations of the comet's orbital motion (Królikowska et al. 1998b). In the orbital version of the model instead of the water production rate derived from the visual magnitudes estimations the function $g(r)$ was used. Values of the model parameters: A, η, I, ϕ, s, f_p could be determined simultaneously with six orbital elements from the observational equations by the least squares method. The forced precession model was successfully employed to modelling the long-term motion of a certain number of short period comets (Sitarski 1995, 1996, Królikowska & Sitarski 1996, Królikowska et al. 1998a).

Sect. 4.3 presents the successfull linkage of all apparitions of the comet 43P/Wolf-Harrington based on the forced precession model in which irregular time shifts of the function $g(r)$ with respect to perihelion were taken into account.

Yeomans & Chodas (1989) modified the symmetrical model of the nongravitational acceleration assuming that the water vaporization curve may reach its peak a certain number of days before or after perihelion. They varied the time shift of the function $g(r)$ with respect to the perihelion passage to find the best fit to the astrometric observations of eight short-period comets. In the asymmetric outgassing model the function $g(r)$, at any time t, is replaced by $g(r')$, where $r' = r(t - \tau)$. Thus, the maximum of the gas production rate is shifted by τ days with respect to the perihelion time. Furthermore, it is worth while to notice that the value of this shift can suffer a change over a long interval of the comet's motion. The method of determination of τ and its constant with time change, $\dot{\tau}$, in a process of the orbit improvement was developed by Sitarski (1994). In this approach the τ displacement is a linear function of time: $\tau = \tau_o + \dot{\tau}(t - t_o)$, where t_o is the osculation epoch of the initial orbit. In many cases the orbital motion of short period comets can be better approximated by the asymmetrical model of the nongravitational acceleration than by the symmetrical one. The Comet 43P/Wolf-Harrington is here a good example (see Sects. 4.2, 4.3).

The perihelion asymmetry of the gas production curve or the cometary light curve can be explained by outgassing from discrete sources on the nucleus surface. For such spotty nucleus, the maximum sublimation rate will take place when the subsolar point is closest to the active region what may not occur at the perihelion passage. Effects of discrete outgassing on the shape of the gas production curve and on nongravitational parameters were discussed in details by Sekanina (1993a, 1993c). In the Sekanina's model, an active region on the surface of a

rotating nucleus experiences diurnal and seasonal variations. The seasonal effects cause the perihelion asymmetry of the gas production curve. Sekanina has shown that for a comet with isolated centres of activity, the sign of A_2 is not related to the direction of nucleus rotation and the nonradial components of the nongravitational acceleration do not vanish even when the lag angle is assumed to be zero. The erratic discontinuities in the nongravitational perturbations of comets or long-term changes in A_2 has been interpreted by Sekanina (1993b) as initiation of new active areas or deactivation of existing ones on the nucleus surface.

The first attempt to introduce the spotty nucleus model directly into the orbital computation was made for the comet 6P/d'Arrest by Szutowicz & Rickman (1993). However, in this approach the observed form of the comet light curve instead of the theoretical gas production curve was used. Actually, the Sekanina's model of discrete sources of a gas emission has been modified and adopted for orbital calculations. Details of the model are presented in Sect. 3. This model with some additional assumptions concerning a lifetime of the active regions, gave satisfactory orbital linkage of all apparitions of the comet 43P/Wolf-Harrington (Sect. 4.4). The spotty nucleus model has been successfully used to link all of observations of comet 46P/Wirtanen assuming temporal variations of the active fraction of the nucleus surface (Szutowicz 1999b, 1999c). The model allowed also to explain a dramatic jump of the nongravitational effects in the motion of the comet 71P/Clark by means of a redistribution of the surface active regions and the change of the nucleus orientation (Szutowicz 1999a).

3. Model of a cometary nucleus with discrete sources of outgassing

The insolation of active regions near the perihelion varies rapidly not only due to variation of the heliocentric distance but also due to changes of the subsolar point latitude. The model of the water ice sublimation for insoled active areas, applied in this study, was formulated by Sekanina (1988). In the model the absorbed solar energy is spent on sublimation and thermal reradiation only. The emission from each active region located on the surface of rotating cometary nucleus is expressed as a product of the water sublimation rate $Z_o(r)$ from the unit area at a subsolar point and the dimensionless relative sublimation rate, $\mid \xi(z_j, r) \mid \leq 1$, at the Sun's local zenith distance z_j $(j = 1, 2, ...N)$. A total number of N sources of outgassing has been assumed. For a small zenith distance of the Sun the relative sublimation rate varies as $\cos z_j$. Its general approximation was given by Sekanina as:

$$\xi(z_j, r) = \begin{cases} \cos z_j - f(r) \sin^2 z_j & 0 \leq z_j \leq z_c \\ 0 & \text{for} \quad z_j > z_c \end{cases}$$

where $f(r)$ is a third order polynomial. The angle z_c is the critical angular distance of the Sun from the active spot, beyond which the sublimation rate is negligibly low as compared with that at the subsolar point and it depends on the $f(r)$. In order to employ the law of sublimation rate in orbital calculations the function $Z_o(r)$ has been normalized to unit heliocentric distance: $Z_o(r) = Z_o(1) \cdot h(r)$, where $Z_o(1) = 1.51836 \cdot 10^{28}$ mol/km^{2}s. Both, function $h(r)$ and widely used in orbital calculations function $g(r)$ have the same form:

$$h(r) = \alpha \left(\frac{r}{r_o}\right)^{-m} \left[1 + \left(\frac{r}{r_o}\right)^{n}\right]^{-k} \tag{3}$$

but $h(r)$ differs in values of the exponents m, n, k and the scale distance r_o, which are equal to 2.1, 3.2, 3.9 and 5.6 AU, respectively. The value of the normalizing constant $\alpha = 0.02726$ was chosen to fill the equation $h(1) = 1$.

Assuming that the variation in orbital position is negligible during one rotation of a cometary nucleus, the rotational-averaged orbital components of the nongravitational acceleration could be described as:

$$a_i = \frac{1}{2\pi} \sum_{j=1}^{N} A_j \; h(r) \int_{-\theta_{cj}}^{\theta_{cj}} \xi(z_j, r) \; C_i \, (\eta, I, \lambda_\odot, \beta_j, \theta_j) \, d\theta_j, \quad i = 1, 2, 3, \tag{4}$$

where C_i are directional cosinus of the momentum transferred to a nucleus by the outgassing from jth source. They depend on the position of active regions and on three angles: η, I, ϕ, characterizing the nuclues as it was described in Sect. 2. The location of the jth discrete center of activity is measured by a cometocentric latitude β_j, positive to the north of the equator and negative to the south, and by an angular distance θ_j from the subsolar meridian. The angle θ_{cj} is the critical hour angle of the Sun at which the sublimation rate from the jth active region reaches minimum or drops to zero during a diurnal cycle. It is related to z_c by: $\cos\theta_{cj} = \cos z_c / \cos\beta_j \cos\delta_\odot - \tan\beta_j \tan\delta_\odot$, where the cometocentric declination of the Sun is defined by: $\sin\delta_\odot = \sin\lambda_\odot \sin I$. For zones which experience days or nights one has $\theta_{cj} = 180^\circ$ or $\theta_{cj} = 0^\circ$, respectively. The constants A_j are given by:

$$A_j = \frac{m\overline{\zeta u}}{M} \, S_j \, Z_o(1), \tag{5}$$

where m is the molecular mass of water, $\overline{\zeta u}$ is the average outflow velocity, S_j is the outgassing area of a jth source and M is the nucleus mass.

For orbital computations the components of the nongravitational acceleration given by Eq. (4) have been transformed into the form:

$$a_i = \sum_{j=1}^{N} A_j \; h(r) \; \langle K_i \, (\eta, I, \lambda_\odot, \beta_j, \theta_{cj}) \rangle \Big|_{t_{1j}}^{t_{2j}}, \quad i = 1, 2, 3 \tag{6}$$

The expressions for $\langle K_i \rangle$ were derived as:

$$\langle K_1 \rangle = C_{\beta_j} \cos\delta_\odot \cos\eta + S_{\beta_j} \sin I \sin\lambda_\odot$$

$$\langle K_2 \rangle = \frac{C_{\beta_j}}{\cos\delta_\odot} (\cos I \sin\eta - \sin^2 I \sin\lambda_\odot \cos\lambda_\odot \cos\eta) + S_{\beta_j} \sin I \cos\lambda_\odot$$

$$\langle K_3\rangle = \frac{C_{\beta_j}\sin I}{\cos\delta_\odot}(\cos I\sin\lambda_\odot\cos\eta+\cos\lambda_\odot\sin\eta) - S_{\beta_j}\cos I$$

where

$$S_{\beta_j} = \frac{\sin\beta_j}{\pi}\,[\cos\delta_\odot\cos\beta_j\sin\theta_{cj}+\theta_{cj}\sin\delta_\odot\sin\beta_j + f(r)(H\ \cos^2\delta_\odot\cos^2\beta_j+\theta_{cj}\ \sin^2\delta_\odot\sin^2\beta_j + \tfrac{1}{2}\ \sin 2\delta_\odot\sin 2\beta_j\sin\theta_{cj}-\theta_{cj})]$$

$$C_{\beta_j} = \frac{\cos\beta_j}{\pi}\,[H\ \cos\delta_\odot\cos\beta_j+\sin\delta_\odot\sin\beta_j\sin\theta_{cj} + f(r)(F\ \cos^2\delta_\odot\cos^2\beta_j+\sin^2\delta_\odot\sin^2\beta_j\sin\theta_{cj} + \tfrac{1}{2}\ H\ \sin 2\delta_\odot\sin 2\beta_j-\sin\theta_{cj})]$$

$$H = \frac{1}{2}\,(\theta_{cj}+\frac{1}{2}\sin 2\theta_{cj})$$

$$F = \sin\theta_{cj}\,(1-\frac{1}{3}\sin^2\theta_{cj}).$$

Lifetime of each active region was limited by time of activation t_{1j} and deactivation t_{2j}.

The expressions (6) were incorporated directly into the equations of the comet's motion (Eq. (1)) which are solved by the recurrent power series method. For the orbit improvement, the method of Sitarski (1971, 1979a, 1979b) was applied. Parameters of the spotty-nucleus model: A_j, η, I, ϕ, and β_j could be simultaneously determined with the orbital elements in the iterative process of the orbit improvement.

4. Nongravitational motion of comet 43P/Wolf-Harrington

The orbital motion of the comet has been investigated based on astrometric observations made during its nine observable apparitions from 1924 to 1998. The total number of the collected observations amounted to 415. From the last return of the comet to the Sun, 212 observations are available. For this dominated apparition the numbers of observations were decreased by taking into account so called normal places i.e. if more than two observations were made at the same day, they were replaced by one average comet position. For each apparition the observations were selected separately according to the mathematically objective criteria elaborated by Bielicki (Bielicki & Sitarski 1991). The mean residuals for each apparition have been calculated. The results from every apparitions have been combined and the "a priori" mean residual of 1.″23, representing accuracy of the whole observational set, was obtained. Global characteristics of the observations are given in Table 1.

4.1. Symmetrical models

The reasonably linkage of all astrometric observations of the comet 43P/Wolf-Harrington was impossible using the standard Marsden's model. This model was explicitly inconsistent with the real motion of the comet giving the mean residual 13.″43.

To examine temporal variations of the nongravitational effects the constant nongravitational parameters A_i, $(i=1,2,3)$ have been determined for each three successive observable apparitions. Values of parameters A_i for such observational intervals are listed in Table 2. The first interval of time has spanned six real apparitions of the comet because it was not observed during its three succesive returns to the Sun after 1924. A particular behaviour of the parametr A_2 connected with the transverse component of the nongravitational force should be noticed. The nongravitational acceleration was slowly decreasing over a long period of time from 1924 to 1978 and then felt down reaching a small value close to zero. It is interesting to see that the acceleration did not switched into deceleration after the 1984 apparition but it started to increase. The parameter A_3 is very poorly determined for almost all intervals of time.

An employment of the model (see Sect. 2) in which A_i are expressed in terms of angular parameters η, I, ϕ of the rotating cometary nucleus allowed to establish the perturbation in the nongravitational motion of the comet as a change in the nucleus orientation. When A_2 increases from negative values to zero, the spin axis of retrograde rotating nucleus approaches the orbital plane. The values of the angular parameters obtained as results of the orbital linkages of four successsive observed apparitions, are presented in Table 3. The parameter ϕ connected with A_3 is rather poorly determined. Unstability in the comet's behaviour around 1984 did not allow to find the solution for the interval 1964–1984. The comet's observations from 1952 to

Table 1. Characteristics of the astrometric observations of 43P/Wolf-Harrington. Observations reduced by normal places are marked by [a].

Perihelion time	Observation interval	No of obs.	No of res.	Mean res.
1925 Jan. 11	1924 Dec. 22 – 1925 Jan. 23	16	28	2.″39
1952 Feb. 6	1951 Oct. 7 – 1952 Apr. 24	39	74	1.″30
1958 Aug. 11	1957 Nov. 18 – 1959 Apr. 10	24	48	1.″10
1965 Feb. 15	1964 Jun. 11 – 1965 Apr. 23	28	55	0.″94
1971 Sep. 1	1970 Nov. 25 – 1972 Apr. 19	25	49	1.″59
1978 Mar. 15	1977 July 11 – 1978 Jan. 17	6	12	3.″04
1984 Sep. 22	1984 Jun. 4 – 1985 Mar. 26	38	76	1.″54
1991 Apr. 4	1990 Jun. 14 – 1991 Mar. 3	27	51	1.″16
1997 Sep. 29	1996 Jun. 15 – 1998 May 26	119[a]	235[a]	0.″57
T o t a l	1924 Dec. 22 – 1998 May 26	322[a]	628[a]	1.″23

Table 2. Nongravitational parameters A_1, A_2, A_3 determined as constant values by linking of each three consecutive observable apparitions of the comet. The mean residuals are given in the last column.

Obs. interval	A_1	A_2	A_3	Mean res.
	10^{-8} AU/day^2			
1924–1959	0.1089 ±.0769	-0.0648 ±.0040	-0.0219 ±.0414	1.″48
1951–1965	0.1995 ±.0380	-0.0513 ±.0012	-0.0486 ±.0246	1.″18
1957–1972	0.3428 ±.0339	-0.0486 ±.0011	-0.0311 ±.0233	1.″27
1964–1978	0.3705 ±.0845	-0.0471 ±.0025	-0.0130 ±.0387	1.″60
1970–1985	0.3335 ±.0558	-0.0096 ±.0028	-0.0002 ±.0374	1.″87
1977–1991	0.2852 ±.1160	-0.0179 ±.0025	-0.0328 ±.0569	1.″86
1984–1998	0.4060 ±.0213	-0.0366 ±.0009	-0.0091 ±.0151	1.″12

Table 3. Angular parameters η, I, ϕ and A of the nucleus of the comet 43P/Wolf-Harrington determined within of sets of four consecutive apparitions. The last interval covers only three returns to the Sun.

Obs. interval	A 10^{-8} AU/day^2	η	I degrees	ϕ	Mean res.
1924–1965	0.319±.022	13.8± 3.1	129.6±13.1	121.6± 27.9	1.″41
1951–1972	0.275±.024	15.6± 4.2	130.1±14.1	144.2± 32.2	1.″31
1957–1978	0.370±.034	10.4± 4.3	135.0±31.1	171.3±131.2	1.″45
1970–1991	0.358±.042	26.4±18.3	95.9± 3.4	258.0± 19.3	1.″82
1984–1998	0.407±.021	10.7± 4.6	118.1±13.5	114.7± 15.2	1.″11

Table 4. Constant nongravitational parameters A_i, $(i = 1, 2, 3)$ and the parameter τ describing the perihelion shift of the function $g(r')$ determined from linkages of each four consecutive apparitions of the comet. The last interval covers three apparitions.

Obs. interval	A_1	A_2 10^{-8} AU/day^2	A_3	τ days	Mean res.
1924–1965	.3441±.0230	-.0296±.0011	.0120±.0248	-26.2± 9.8	1.″41
1951–1972	.3085±.0312	-.0322±.0064	-.0446±.0168	-22.4± 8.0	1.″29
1957–1978	.3558±.0358	-.0520±.0088	-.0360±.0244	4.3± 8.0	1.″45
1964–1985	.0966±.0360	-.0327±.0075	.0328±.0248	14.1± 3.1	1.″98
1970–1991	.3668±.0380	-.0173±.0122	-.0407±.0298	4.1±11.2	1.″83
1984–1998	.3605±.0217	-.0193±.0074	-.0055±.0142	-16.8± 8.3	1.″10

1991 have been linked previously (Szutowicz 1992) assuming linear variations of the angles I and ϕ. Unfortunately, fitting of all apparitions of the comet to this model has failed.

4.2. Asymmetrical model

Asymmetrical model of the nongravitational acceleration understood as a perihelion shift of the function $g(r)$ (see Sect. 2) provided a much better orbital solution than the standard model. The orbital linkage of all comet's apparitions with the mean residual equal to $1.''85$ was obtained. However, it was necessary to introduce a linear variation of two parameters: the τ describing the time shift of $g(r)$ with respect to the perihelion and the angle ϕ connected with the comet's orientation. According to this orbital fit the function $g(r')$ reached peak 23 days before perihelion passage in 1925 and due to the linear evolution its maximum occured about 57 days after perihelion of the 1997 apparition. Linear variations of parameters remarkably limit the physical meaning of the model especially for the prediction of the future orbit.

To study a behaviour of the perihelion shift of $g(r')$ in shorter intervals of time, the asymmetric model was applied for each four successively observable apparitions of the comet. In Table 4, the values of A_i and τ in the appropriate observational intervals are presented. The last interval includes only three apparitions, because of difficulty in linking of the observations from 1977 to 1998. One can see that a form of A_2 variations is different than that for the symmetrical model. The maximum of the function $g(r')$ significantly peaks before perihelion passages for the comet's returns until the 1972. Then the acceleration decreases and the parameter τ reaches positive values. The second change of τ takes place after the 1991 apparition and the maximum of $g(r')$ is shifted again before perihelion. Nonlinear variations of τ explain the poor accuracy of the orbital linkage of all comet's observations where the linear change of τ was assumed. However, a general evolution of the shift of the maximum cometary activity, from negative to positive number of days in consecutive returns of the comet, has been confirmed.

4.3. Forced precession model

The analysis of the nongravitational parameters determined as constant values within sets of three or four consecutive apparitions has shown long-term variations of the nongravitational perturbations in the orbital motion of Comet Wolf-Harrington. One of the posssible explanation of these temporal variations could be forced precession of a rotating nonspherical cometary nucleus. Therefore the orbital version of the forced precession model (see Sect. 2) was applied. The model has been preliminary employed to link all of the comet apparitions (Królikowska et al. 1998a), where the last return was represented by observations made only till December 1997. Values of six model parameters has been found for a prolate spheroid nucleus of the comet. The comparison of the mean residual of that orbital solution which reached $2.''26$ with the 'a priori' residual of $1.''26$ indicated that the forced precession model needs some additional parameters to give better approximation to the real motion of the comet. As it follows from Table 2 the nongravitational perturbations exibit some irregular behaviour represented by unexpected changes not only in A_i but in τ, too. Time shift of the function $g(r')$ described by τ can be determined together with the basic parameters of the forced precession model. To model discontinuities in the nongravitational motion of the comet changes of values of τ close to the selected moments of aphelion passage has been assumed. After some numerical calculations two moments of discontinuities in 1975 and in 1988 has been established. The model parameters: A, η, I_o, ϕ_o, f_p, s, τ_1, τ_2, τ_3 as well as orbital elements were determined together in a process of the iterative improvement of the orbit. All parameters are listed in Table 5 as Model C. The orbital solution was fitted to all observations of the comet with the mean residual of $1.''39$. According to the model, the nucleus is a slightly prolated spheroid with the ratio of the longer axis to shorter one being equal to 1.05 ± 0.02. Precessional variations of the equatorial obliquity, I, and the solar longitude at the perihelion, ϕ, during 72 years of the comet's motion are shown in Fig. 1. Time dependences of the acceleration's orbital components a_1, a_2, a_3 during the same interval of time are presented in Fig. 2. They are compared with appropriate evolutions of a_i obtained from the orbital solution for the spotty nucleus (Model A).

Based on discontinuities in the nongravitational perturbations the comet 43P/Wolf-Harrington may be classified as an "erratic" comet. Its orbital motion was compared with that of five comets which exhibit strongly variable nongravitational effects (Królikowska et al. 1999, 2000). The satisfactory precessional models were found for all of these comets.

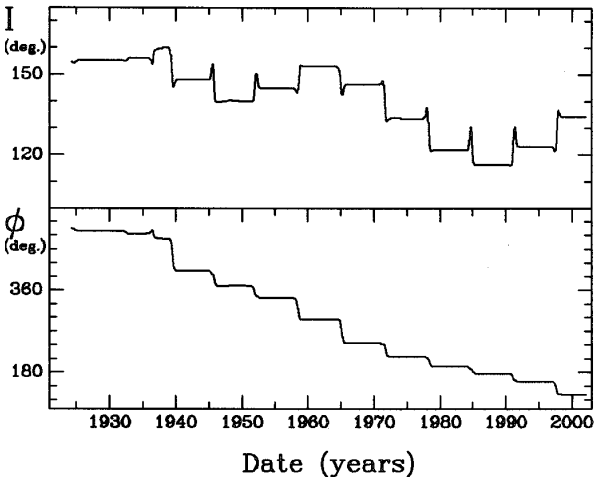

Fig. 1. Temporal variation of angles I and ϕ for Comet 43P/Wolf-Harrington due to the spin-axis forced precession of the comet's nucleus.

Table 5. Parameters describing the comet nucleus and the orbit obtained from fitting the forced precession model to all positional observations of the comet 43P/Wolf-Harrington

Model C		mean residual: 1.″39	
A $(10^{-8}$ AU/day$^2)$	η	I	ϕ
0.36343±.00612	6.°36±0.°41	125.°05±4.°40	143.°47±14.°80
s	f_p $(10^7$ AU/day)		
-0.04506±.01994	-0.31357±.06697		
τ (days)			
-17.782±1.752	$t \leq$ 1975 Jan. 01		
8.394±0.824	for 1975 Jan. 01 $< t \leq$ 1988 Jan. 06		
-11.691±0.884	$t >$ 1988 Jan. 06		
Orbital elements;	*Equinox: J2000.0*		
Epoch: 1997 Sep. 29	T: 1997 Sep. 29.21850		
q: 1.58182646 AU	e: 0.54394750		
ω: 187.°13349	Ω: 254.°75651	i: 18.°51059	

4.4. Spotty nucleus model

Time dependent shifts of a maximum activity seem to play essential role in the nongravitational motion of the comet Wolf-Harrington. Attemps to model the nongravitational acceleration as a result of the outgassing from one emission source which is active in the same degree over the whole interval motion of the comet 43P/Wolf-Harrington, have not been successful even taking into account a linear precession of the spin axis. Extensive numerical experiments with using a model of the spotty-nucleus described in Sect. 3, allowed to ascertain that processes of activation and/or deactivation of emission sources on the nucleus surface took place at least three times. From numerical fitting of the model parameters to positional observations, the lag angle, η, the orientation of the nucleus in space described by the angles I and ϕ, the localization of three active regions given by cometocentric latitudes, $\beta_I, \beta_{II}, \beta_{III}$, and appropriate values of the A_I, A_{II} A_{III} parameters have been derived. Two orbital solutions called Model A and Model B were found on the assumption of slightly different lifetimes of active regions. In Table 6 both solutions are represented by the model parameters and orbital elements. Time of activation and deactivation of the regions are given too. The models have been satisfactory fitted to real motion of the comet, with the same mean residual of 1.″39 as in the case of the precessional model. From presented solutions follows that the appearance and disappearance of regions located on the southern hemisphere of the comet nucleus are resposible for the variation of the nongravitational behaviour of the comet.

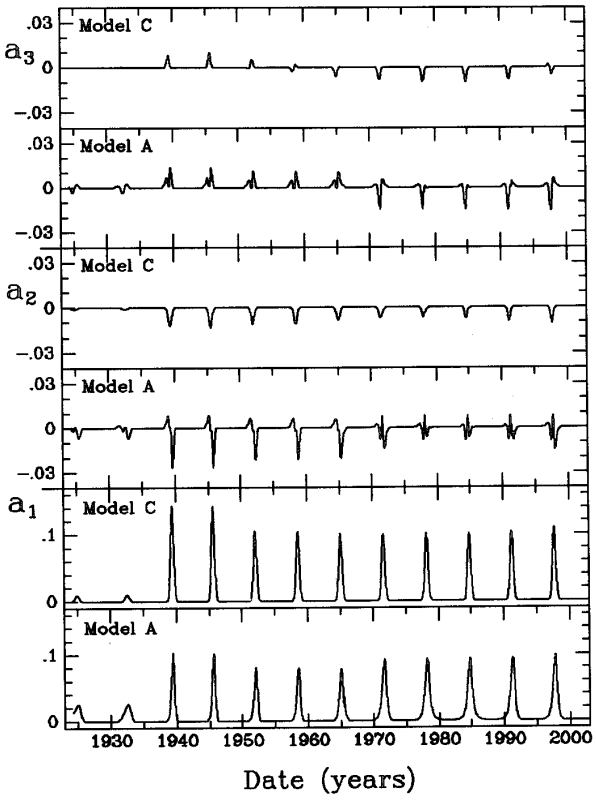

Fig. 2. Orbital components a_i of the nongravitational acceleration as functions of time for 43P/Wolf-Harrington obtained from dicrete outgassing model (Model A) and forced precession model (Model C)

In both cases the first region (I) is situated on the northern hemisphere of the nucleus at the latitude of about $+37°$. It was found to be the largest and persistent active, whereas on the southern hemisphere the variations of activity have been discovered. The second region (II), which was localized near to the cometary equator, became active about 150 days after perihelion of the 1965. According to scenario related to the Model A the total active area increased once again before 1978 apparition due to activation of the third region (III) on the latitude of $-51°$. This region decayed about 160 days after perihelion passage of the 1991. While from the Model B follows that the second region vanished after perihelion in 1978 and the third one was localized nearer to the equator than the analogue region of Model A.

Taking into account that the activation of new regions could disturb the nucleus spin axis, the orbital programme was run to

Table 6. Physical parameters of the nucleus and orbital elements obtained from linking all apparitions of the comet 43P/Wolf-Harrington by using of discrete outgassing model. Two possible orbital solutions called Model A and Model B are presented. The active regions are denoted by I, II, III.

	Model A	**Model B**
η	$2\overset{\circ}{.}15 \pm 0\overset{\circ}{.}29$	$1\overset{\circ}{.}87 \pm 0\overset{\circ}{.}40$
I_o	$117\overset{\circ}{.}28 \pm 3\overset{\circ}{.}04$	$112\overset{\circ}{.}96 \pm 3\overset{\circ}{.}25$
ϕ_o	$117\overset{\circ}{.}55 \pm 0\overset{\circ}{.}97$	$117\overset{\circ}{.}36 \pm 0\overset{\circ}{.}87$
β_I	$38\overset{\circ}{.}86 \pm 1\overset{\circ}{.}62$	$35\overset{\circ}{.}82 \pm 1\overset{\circ}{.}12$
A_I $(10^{-8}\,\mathrm{AU/day^2})$	0.65972 ± 0.03476	0.72497 ± 0.03148
activity time:	1924–1998	1924–1998
β_{II}	$-3\overset{\circ}{.}53 \pm 1\overset{\circ}{.}55$	$-4\overset{\circ}{.}88 \pm 2\overset{\circ}{.}88$
A_{II} $(10^{-8}\,\mathrm{AU/day^2})$	0.59792 ± 0.09475	0.51734 ± 0.11982
activity time:	1965 June 14–1998	1965 June 14 - - 1978 Nov. 30
β_{III}	$-51\overset{\circ}{.}38 \pm 5\overset{\circ}{.}24$	$-31\overset{\circ}{.}41 \pm 1\overset{\circ}{.}93$
A_{III} $(10^{-8}\,\mathrm{AU/day^2})$	0.39489 ± 0.01796	0.62595 ± 0.02825
activity time:	1977 June 15 - - 1991 Sep. 15	1978 Aug. 1 - - 1991 Sep. 15
Orbital elements; Equinox: J2000.0		
Epoch:	1997 Aug. 20	1997 Aug. 20
T	1997 Sep. 29.21850	1997 Sep. 29.21835
q (AU)	1.58182559	1.58182786
e	0.54394559	0.54394824
ω	$187\overset{\circ}{.}13373$	$187\overset{\circ}{.}13371$
Ω	$254\overset{\circ}{.}75623$	$254\overset{\circ}{.}75624$
i	$18\overset{\circ}{.}51062$	$18\overset{\circ}{.}51061$
mean residual	$1\overset{''}{.}39$	$1\overset{''}{.}39$

search for the possible change of the angles I and ϕ. Solution with the discontinuity in the equatorial obliquity around 1978 was found. However, the mean residual did not change in spite of introducing new parameters, therefore the new solution was given up.

In Fig. 2 variations of three orbital components of the non-gravitational acceleration during the whole investigated period of the comet's motion resulting from the Model A are shown. One easily recognizes that in the case of the forced precession model the component a_2 is always negative or close to zero, whereas for the spotty - nucleus model a_2 is strongly variable near perihelions and reaches either positive and negative values.

5. Evolution of the orbit

As a solution for prediction of the future orbit, the Model A with the discrete emission sources on the nucleus surface was chosen. Using this model the evolution of the comet orbit during 1924–2010 was investigated. Equations of the comet motion have been integrated including all planetary perturbations. The orbital elements for all perihelion times are listed in Table 7. The apparitions from which observations were performed are denoted by asterisks. The comet experienced two close encounters with Jupiter between the 1924 apparition and the 1951 one. After the first approach in June 1936 at the distance of 0.123 AU, the perihelion distance was reduced from 2.42 to 1.45 AU and the orbital period dropped from 7.6 to 6.2 years. The second approach in January 1948 at 0.716 AU caused opposite changes but much smaller than the first one. The comet once again will decrease the distance to the Sun at perihelion of the 2010 apparition shortening the orbital period to 6.1 years due to approach Jupiter in June 2007. The orbit evolution is plotted in Fig. 3.

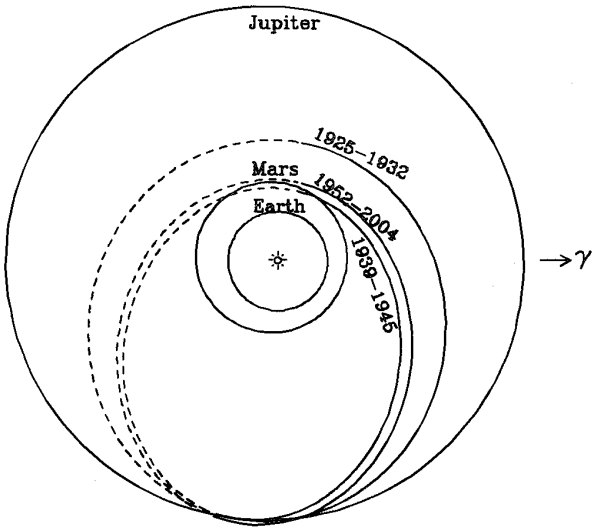

Fig. 3. The orbit evolution between 1925 and 2004

6. Activity of the comet

6.1. Observed light curves

Additional information and an independent test for the orbital solutions follow from observable light curves. Information on the total brightness of the comet is rather poor. A small number of observers and observations must be due to the comet's faintness (peak magnitude $\sim 11^m$). The analysis of the comet's brightness in the period 1924–1984 was based on The *Comet Light Curve Catalogue/Atlas* (Kamel 1991). The catalogue contains reduced magnitudes, corrected for the geocentric distance. For photographic observations a colour correction is used. In the case of the comet Wolf-Harrington, magnitudes are additionaly corrected for observational effects, e.g. the sky brightness and altitude. During the first discovery apparition in 1924 the comet was observed very shortly and remained very faint, never becoming brighter than $15th$ magnitude. There are only four total brightness estimates from the 1958, 1965 and 1978 apparitions. In that case the four apparitions mentioned above have been omitted in the analysis of the comet's light curves. The light curves extracted from the Catalogue for the 1951, 1971 and 1984 apparitions are represented by 25, 7 and 20 magnitude estimates, respectively, all made by 21 observers. The magnitude data used in the study of the comet's brightness in the 1991 and 1997 apparitions were reported in *The International Comet Quarterly* (Numbers 77–80; 101, 103–107) by 6 and 26 observers, respectively. The total number of magnitude estimates was 39 for 1991 and 85 for 1997. To construct the light curves,

Table 7. The evolution of the orbital elements according to the Model A given in Table 6; perihelion distance q is in AU, period P is in years, angular parameters ω, Ω, i are referred to J2000.0. The apparitions which have been observed and used for the orbit improvement are denoted by an asterisk.

	T (ET)	q	e	P	ω	Ω	i	Epoch
*	1925 Jan. 11.3660	2.428411	0.371657	7.60	180.°2079	261.°3867	23.°6842	1925 Jan. 11
	1932 Aug. 14.5667	2.416234	0.372998	7.56	180.°4043	261.°3272	23.°7143	1932 Aug. 14
	1939 June 25.6493	1.447732	0.570822	6.20	184.°4030	256.°1279	18.°3227	1939 June 25
	1945 Sep. 9.0355	1.449976	0.570489	6.20	184.°5477	256.°0704	18.°3143	1945 Sep. 9
*	1952 Feb. 6.6838	1.599103	0.540669	6.50	186.°8864	254.°9937	18.°4933	1952 Feb. 6
*	1958 Aug. 11.4201	1.604496	0.539864	6.51	187.°0075	254.°9426	18.°4779	1958 Aug. 11
*	1965 Feb. 15.5507	1.614447	0.538107	6.53	186.°9999	254.°9324	18.°4581	1965 Feb. 15
*	1971 Sep. 1.1779	1.621819	0.536762	6.55	186.°9926	254.°9178	18.°4331	1971 Sep. 1
*	1978 Mar. 15.8944	1.614588	0.537996	6.53	186.°9621	254.°9305	18.°4578	1978 Mar. 15
*	1984 Sep. 22.7554	1.615896	0.537725	6.54	186.°8417	254.°9283	18.°4478	1984 Sep. 22
*	1991 Apr. 4.8295	1.607837	0.539041	6.51	186.°9529	254.°8900	18.°4721	1991 Apr. 4
*	1997 Sep. 29.2172	1.581827	0.543976	6.46	187.°1330	254.°7563	18.°5104	1997 Sep. 29
	2004 Mar. 17.8454	1.578634	0.544594	6.45	187.°2748	254.°6945	18.°5205	2004 Mar. 17
	2010 July 1.7126	1.357667	0.594435	6.12	191.°4694	249.°8974	15.°9681	2010 July 1

all of the available data were used and they were reduced to 1 AU geocentric distance. The small number of estimates provided by each observer did not allow to find the systematic personal errors. Furthermore, no corrections for telescope apperture were applied. All derived light curves are presented in Fig. 4 as the heliocentric magnitudes versus time from the perihelion passage. The magnitude data are marked with open circles. The solid and dashed lines are the theoretical light curves obtained on the basis of the orbital solutions.

6.2. Theoretical light curves

To compare the observed brightness variations of the comet with the modeled profile of its activity the Model A and Model B have been applied. For each active region the rotational-averaged water sublimation rates per unit surface area (km^2):

$$\langle Z\rangle_j = \frac{1}{2\pi}\int_{-\theta_{cj}}^{\theta_{cj}} Z_o(r)\ \xi(z_j,r)d\theta_j, \quad j = I, II, III \tag{7}$$

have been derived over each orbit under consideration. The averaged sublimation rates for the whole comet nucleus are as follow:

$$\langle Z\rangle = \frac{\sum_{j=I}^{III}\langle Z\rangle_j\ A_j}{A_c}, \tag{8}$$

where $A_c = \sum_{j=I}^{III} A_j$. The constants A_j derived from orbital calculations are given in Table 6. If the appropriate region was inactive at any time then $A_j = 0$. The profiles of the outgassing curves for the Model A are shown in Fig. 5 as the logarithm of the modeled sublimation rates $\langle Z\rangle$ versus time to perihelion in successive apparitions. Variations of shapes are evident due to initiation and deactivation of the regions and evolution of the orbit as well. One can see that until the 1971 apparition the maxima occured before perihelion passages, for 1984 and 1991 apparitions they fall clearly after perihelion but during the last return of the comet the shift was slightly negative again.

Next, $\langle Z\rangle$ was transformed into the total water production rate, Q, expressed in molecules per second, using the relation: $Q = \langle Z\rangle\ S_c$, where S_c is the total outgassing area. In the other words the vertical shift between the Q and $\langle Z\rangle$ yields the active area on the comet surface. Finally the water production rate was related to the heliocentric magnitude. The empirical law in the form of linear dependences between the logarithm of the production rate and the visual magnitude were proposed by several authors (Jorda et al. 1992, Festou 1986, Sekanina 1989). For the comet P/Wolf-Harrington there is a possibility to verify this relationship because OH production rates derived from the narrow-band photometry are available (Schleicher et al. 1993). The four pre-perihelion $logQ_{OH}$ estimates from the 1991 and one post-perihelion data from the 1984 combine with the observed brightness of the comet were used to establish the first coefficient in the calibration formula:

$$logQ_{H_2O} = 30.47 - 0.24 m_H \tag{9}$$

The second coefficient comes from Jorda et al. (1992) and is close to the value usually used. The water production rate is related to the OH production rate by: $Q_{H_2O} = 1.1 Q_{OH}$. Five water sublimation estimations given by Schleicher et al. were converted into m_H and marked with triangles in Fig. 4. Theoretical light curve can be express by:

$$m_H^T = \frac{30.47 - \log[\langle Z\rangle\ S_c]}{0.24} \tag{10}$$

The shape of the m_H^T curve is determined by an insolation pattern in each apparition but their amplitude depends on the outgassing area as well. To establish the total size of the active area, S_c, the level of the observed and theoretical light curve should be compared. The theoretical light curve from 1991 was scaled by an active area to reach the observed level of the comet's brightness in this apparition. In a result for S_c was adopted value of 3.76 km^2 (Model A) and 4.90 km^2 (Model B). The total outgassing area is a sum of areas of every regions ($S_c = \sum_{j=I}^{III} S_j$)

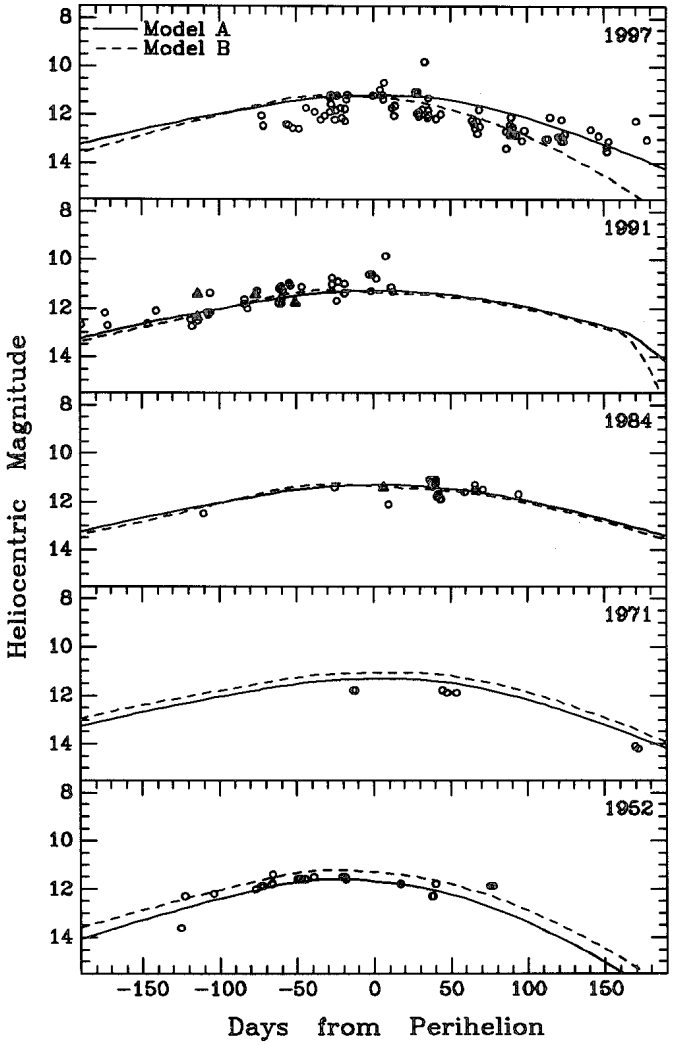

Fig. 4. Heliocentric magnitude of the comet 43P/Wolf-Harrington for the 1952, 1971, 1984, 1991 and 1997 apparitions. The observed brightnesses are marked with open circles. The water production rate, Q, converted into m_H are shown with full triangles. The theoretical light curves derived from Model A and B for the spotty nucleus are plotted with solid and dashed lines, respectively.

and on the other hand: $S_c = \frac{S_j}{A_j} A_c$. Thus it is possible to determine the area of each active spot on the nucleus and the variation of S_c in the successive apparitions, too. The appropriate total outgassing areas, S_c are given in Table 8. Taking into account these values, the variations of the comet brightnesses m_H^T could be calculated from Eq. (10). They are plotted in Fig. 4 by solid and dashed lines for Model A and Model B, respectively. To compare the observed and theoretical light curves the apparitions 1951, 1971, 1984, 1991 and 1997 with known brightness estimates have been chosen only. It should be noticed that theoretical curves are fitted quite well to observed ones.

The shifts of maxima of the brightness curves with respect to perihelion in the successive returns of the comet, τ_a, and their maximum values $m^T_{H_{max}}$ measured in magnitudes are listed in Table 8. In Columns 5 (Model A) and 10 (Model B) the activity

Table 8. Maxima of the theoretical light curves measured in magnitudes and its time shift respect to successive perihelions between 1924 and 2010 with corresponding to them the total ougassing areas and the active fractions of the nucleus calculated for the radius nucleus amounted to 1.07 km (Model A) and 1.12 km (Model B).

	Model A				Model B			
App.	$m^T_{H_{max}}$ mag.	shift days	S_c km^2	f_a	$m^T_{H_{max}}$ mag.	shift days	S_c km^2	f_a
1925	13.77	-39.3	1.50	0.11	13.47	-20.8	1.90	0.13
1932	13.73	-41.6	1.50	0.11	13.44	-21.0	1.90	0.13
1939	11.08	-20.3	1.50	0.11	10.73	-21.1	1.90	0.13
1945	11.09	-21.1	1.50	0.11	10.74	-21.5	1.90	0.13
1952	11.55	-27.6	1.50	0.11	11.20	-25.6	1.90	0.13
1958	11.57	-28.0	1.50	0.11	11.22	-26.2	1.90	0.13
1965	11.60	-26.6	1.50	0.11	11.25	-26.0	1.90	0.13
1971	11.27	7.2	2.86	0.21	11.04	11.7	3.26	0.23
1978	11.25	6.5	3.76	0.28	11.02	11.9	3.26	0.23
1984	11.26	6.7	3.76	0.28	11.25	-25.8	4.90	0.35
1991	11.23	6.2	3.76	0.28	11.23	-24.1	4.90	0.35
1997	11.16	6.3	2.86	0.21	11.15	-24.8	1.90	0.13
2004	11.12	6.6	2.86	0.21	11.14	-25.7	1.90	0.13
2010	10.47	5.9	2.86	0.21	10.48	-20.1	1.90	0.13

level understood as the fraction of the total surface participating in the outgassing were given. The active fractions were calculated from the expression $f_a = \frac{S_c}{4\pi R^2}$. For the nucleus radius, R, the values 1.07 km (Model A) and 1.12 km (Model B) were assumed (see Sect. 7).

7. The nucleus radius

The upper limit on the comet radius can be obtained from photometry of the nuclear condensation. If there is no coma around the cometary nucleus then the absolute magnitude H_N given by Rickman (1992):

$$H_N = 14.10 - 2.5 \log p_v - 5 \log R \tag{11}$$

allows directly to estimate the radius of the bare nucleus knowing its geometric albedo p_v. The absolute magnitude of a comet can be obtained from the observed nuclear magnitude m_2 reduced to unit geocentic, Δ, and heliocentric distance and zero degree phase i.e.

$$H_N = m_2 - 5 \log r\Delta - \beta\alpha. \tag{12}$$

The α is the phase angle at the time of observation and the phase coefficient, β, is usually taken to be 0.035 Jewitt & Luu (1992).

The nuclear magnitudes of the comet 43P/Wolf-Harrington from the period 1951–1978 employed in this study come from the Kamel's Catalogue. A large number of nuclear magnitudes were reported by Roemer and her collaborators (33 data points from the 1958, 1965 and 1971 apparitions) and a few ones by Mrkos & Schwarz. The five observations in 1951–1952 were obtained by Cuningham et al. The data have been supplemented with estimates made by Hainaut et al. (MPC 27955), Offut (MPC 27955), Scotti (MPC 27955, ICQ 107), Hergenrother (ICQ 100)

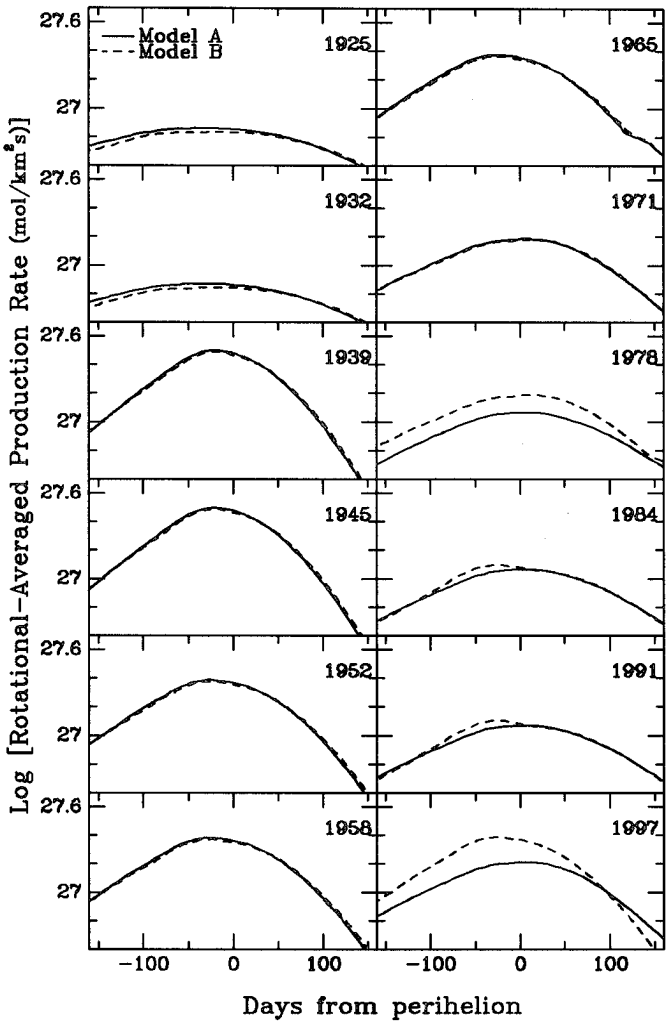

Fig. 5. Rotational-averaged water sublimation rate in function of the perihelion time derived from Model A and B for all apparitions of comet 43P/Wolf-Harrington.

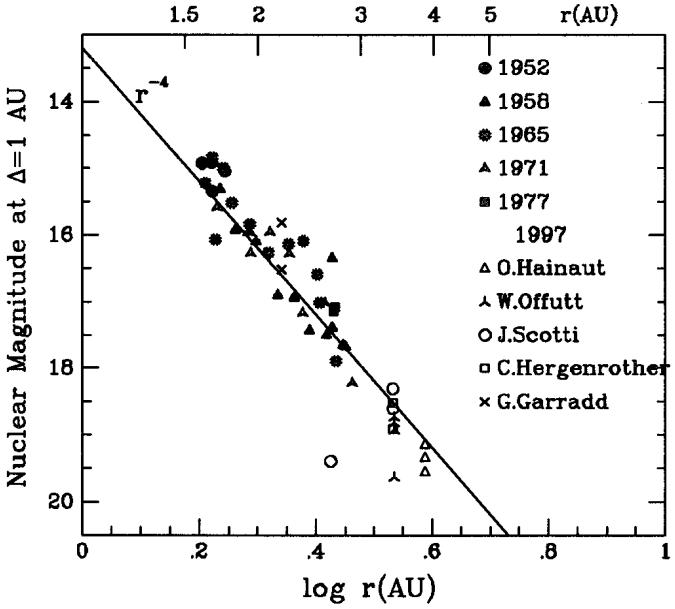

Fig. 6. The nuclear brightnesses of the comet in 1952, 1958, 1965, 1971, 1977 and 1997 apparition versus log r.

& Garradd (MPC 31329) in 1996 and 1998. The collected nuclear magnitudes have been normalized to a geocentric distance of 1 AU and plotted against $\log r$ in Fig. 6.

The magnitude estimates follows an inverse fourth power law heliocentric distance therefore they are inconsistent with reflection from a bare nucleus, suggesting that the coma is still present. To avoid possible contamination by products of the comet's activity the observations at a large heliocentric distance should be taken into account. Employing three estimations of the comet's magnitude at a heliocentric distance of 3.87 AU, made during the last apparition, the H_N were calculated from Eq. (12) and next assuming a geometric albedo of 0.04, the mean nucleus radius was computed from the Eq. (11) as being equal to 2.09 km. Slightly smaller radius of 1.64 km was obtained on the basis on the observations at 3.4 AU and 2.6 AU. On the base photometric observations made at a heliocentric distance of 4.87 AU Lowry et al. (1999) estimated the nuclear radius of the comet on 3.3 km.

In the further analysis of the constraints on the comet nucleus, the nongravitational acceleration was involved. The equation: $M = \frac{m\zeta u}{A_c} S_c Z_o(1)$ allows directly to calculate the mass of the comet nucleus, knowing values of the S_c. Assuming effective outflow velocity of the pure H_2O as equal to 0.3 km s^{-1}, the nucleus mass amounted to $(1.5445 \pm 0.0831) \cdot 10^{12}$ kg (Model A) and $(1.7803 \pm 0.0773) \cdot 10^{12}$ kg (Model B). On the other hand the nucleus mass is related to R by: $M = \rho \frac{4}{3}\pi R^3$. Assuming the bulk density on 0.3 g/cm^3 or 0.5 g/cm^3 the nucleus radius was evaluated as 1.07 ± 0.02 km or 0.90 ± 0.02 km (Model A) and 1.12 ± 0.02 km or 0.95 ± 0.02 km (Model B). The reliability of these estimations is limited by the assumed theory of sublimation.

8. Discussion

Orbital investigation allows to verify models of the nongravitational forces by comparing model of the perturbed motion of a comet with its real position on the orbit described by astrometric observations.

In all presented models of the nongravitational acceleration perturbing the orbital motion of the comet 43P/Wolf-Harrington the similar evolution of the time shift of maximum activity with respect to perihelion was detected. This temporal evolution over the whole examined interval of the comet's motion derived from three different kind of models was presented in Fig. 7. For the forced precession model the time displacements of the function $g(r)$ with respect to the perihelion described by parameters τ_1, τ_2 and τ_3 (Table 5) are presented as straight solid lines. Shifts of the maximum outgassing related to seasons effect resulting from Model A and Model B (Table 8) for the spotty nucleus model are marked in each apparition with big circles full and open, respectively. The character of variations of the activity

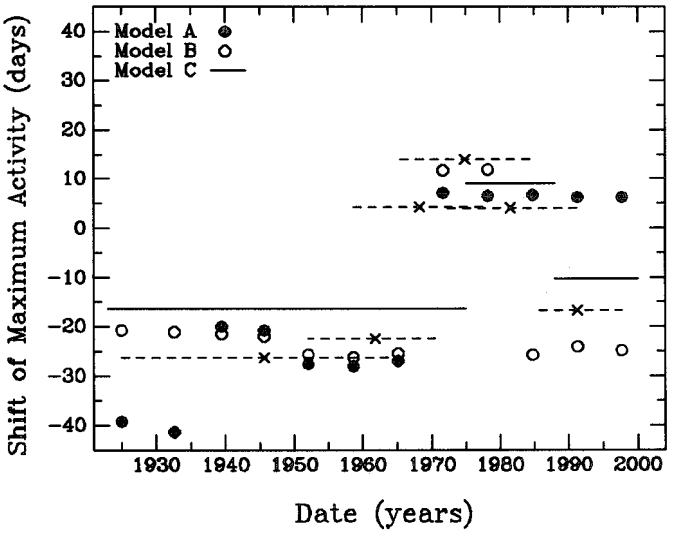

Fig. 7. Time shift of the maximum activity with respect to the perihelion in the successive apparitions of the comet 43P/Wolf-Harrington obtained from different models. Dashed lines with centers denoted by crosses present the values of τ found from orbital linkages of three consequtive apparitions by the asymmetrical model of the nongravitational acceleration. The values of parameters τ_1, τ_2 and τ_3 determined from linkage of all apparitions by forced precession model (Model C) are drawn as straight solid lines. The perihelion shift of the gas production curves derived from the model of discrete outgassing from the nucleus surface are presented by full circles for Model A and open circles for Model B.

shift which was originally negative then positive and again negative in the last apparition has been independently confirmed by three different models. Two of them represented by Model A, Model B and Model C successfully linked all apparitions of the comet. The third one was the asymmetric model used within short intervals of time covering three or four apparitions. The appropriate values of parameters τ (Table 4) are drawn in Fig. 7 by straight dashed lines with crosses in the centres.

From the present investigation follows that variations in the standard nongravitational parameter A_2, can be interpreted as manifestations of a sudden redistribution of the momentum that is transferred to the nucleus by the sublimating mass. According to orbital solutions for the spotty nucleus an episodic activation of new emission region and deactivation of the existing one are responsible for the momentum changes. Likewise in a case of the forced precession model stepwise variations of the maximum function $g(r)$ with respect to perihelion have been obtained.

The outgassing pattern may be affected by changes in the surface insolation distribution. For a nonspherical nucleus the spin axis is forced to precess when the momentum transfered to the nucleus does not pass through the center of mass. Sekanina (1993b) pointed out that due to the nucleus precession the dormant sources of activity may be exposure to sunlight and simultaneusly the active regions may be protected from insolation. Exposition to sunlight of new sources of outgassing can, in turn, exert a torque that sustain nucleus precession. The irregular changes of the time shifts of $g(r)$ with respect to perihelion, obtained on the basis of the forced precession model can be interpreted as variations in the localizations of the active areas on the nucleus of the comet 46P/Wolf-Harrington. The variations in distribution of the active areas on the nucleus surface cause both the horizontal shifts and amplitude changes of the outgassing curves. Unfortunately the presented precessional model for uniform distribution of the active areas on the nucleus surface offers the perihelion shifts of the symmetrical production curve only. Probably the comet 43P/Wolf-Harington needs a model of the forced precession for the nucleus with activity concentrated in localized sources on the surface. Nevertheless, it seems that scenarios of the activity variations proposed here can explain the temporal variability of the nongravitional perturbations in the long-term of the comet's motion and are consistent if the variations of the shift perihelion of activity are considered.

Orbital investigation allows to verify models of the nongravitational forces by comparing model of the perturbed motion of a comet with its real position on the orbit described by astrometric observations.

Acknowledgements. This work was partially supported by the Polish Committee of Scientific Research (K.B.N. grant number 2 P03D 002 09).

References

Bielicki M., Sitarski G., 1991, Acta Astron. 41, 309
Festou M.C., 1986, In: Lagerqvist C.-I., Lindblad B.A., Lundstedt H., Rickman H. (eds.) Asteroids Comets Meteors II, p. 299
Jewitt D.C., Luu J.X., 1992, Icarus 100, 187
Jorda L., Crovisier J., Green D.W.E., 1992, In: Harris A.W., Bowell E. (eds.) Asteroids, Comets, Meteors, p. 285
Kamel L., 1991, The Comet Light Curve Catalogue/Atlas. Part I and II
Królikowska M., Sitarski G., 1996, A&A 310, 992
Królikowska M., Sitarski G., Szutowicz S., 1998a, Acta Astron. 48, 91
Królikowska M., Sitarski G., Szutowicz S., 1998b, A&A 335, 757
Królikowska M., Sitarski G., Szutowicz S., 1999, In: Svoren J., Pittich E.M., Rickman H. (eds.) Proc. of the IAU Coll. 173, p. 381
Królikowska M., Sitarski G., Szutowicz S., 2000, in preparation
Lowry S.C., Fitzsimmons A., Cartwright I.M., Williams I.P., 1999, A&A 349, 649
Marsden B.G., 1977, IAU Circ. 3074
Marsden B.G., Sekanina Z., Yeomans D.K., 1973, AJ 78, 211
Rickman H., 1992, In: Benest D., Froeschle C. (eds.) Interrelations between Physics and Dynamics for Minor Bodies in the Solar System. p. 197
Schleicher D.G., Bus S.J., Osip D.J., 1993, Icarus 104, 157
Sekanina Z., 1981, Ann. Rev. Earth. Planet. Sci. 9, 113
Sekanina Z., 1984, AJ 89, 1573
Sekanina Z., 1985a, AJ 90, 827
Sekanina Z., 1985b, AJ 90, 1370
Sekanina Z., Yeomans D.K., 1985, AJ 90, 2335
Sekanina Z., 1988, AJ 95, 911
Sekanina Z., 1989, AJ 98, 2322
Sekanina Z., 1993a, AJ 105, 702
Sekanina Z., 1993b, A&A 271, 630
Sekanina Z., 1993c, A&A 277, 265
Sitarski G., 1970, Acta Astron. 20, 271

Sitarski G., 1971, Acta Astron. 21, 87
Sitarski G., 1979a, Acta Astron. 29, 401
Sitarski G., 1979b, Acta Astron. 29, 413
Sitarski G., 1981, Acta Astron. 31, 471
Sitarski G., 1990, Acta Astron. 40, 405
Sitarski G., 1994, Acta Astron. 44, 91
Sitarski G., 1995, Acta Astron. 45, 763
Sitarski G., 1996, Acta Astron. 46, 29
Szutowicz S., 1987, Acta Astron. 37, 179
Szutowicz S., 1992, In: Brahic A., Gerard J.-C., Surdej J. (eds.) Proc. of the 30th Liege Int. Astroph. Colloquium, p. 371
Szutowicz S., 1999a, In: Svoren J., Pittich E.M., Rickman H. (eds.) Proc. of the IAU Coll. 173, p. 259
Szutowicz S., 1999b, In: Asteroids, Comets, Meteors (abstract)
Szutowicz S., 1999c, Ph.D. Thesis, in polish
Szutowicz S., Rickman H., 1993, In: Kurzynska K., Barlier F., Seidelmann P.K., Wytrzyszczak I. (eds) Proc. of the Conf. on Astrometry and Celestial Mechanics, p. 425
Whipple F.L., Sekanina Z., 1979, AJ 84, 1894
Wiśniewski W., 1964, Acta Astron. 14, 130
Yeomans D.K., Chodas P.W, 1989, AJ 98, 1083